HHS Public Access

Author manuscript

ACS Catal. Author manuscript; available in PMC 2022 August 20.

Published in final edited form as:

ACS Catal. 2021 August 20; 11: 10308–10315. doi:10.1021/acscatal.1c02750.

GH47 and Other Glycoside Hydrolases Catalyze Glycosidic Bond Cleavage with the Assistance of Substrate Super-arming at the Transition State

Jonathan C. K. Quirke[a,b,c], **David Crich**[a,b,c]

[a)]Department of Pharmaceutical and Biomedical Sciences, University of Georgia, 250 West Green Street, Athens, GA 30602, USA

[b)]Department of Chemistry, University of Georgia, 140 Cedar Street, Athens, GA 30602, USA

[c)]Complex Carbohydrate Research Center, University of Georgia, 315 Riverbend Road, Athens, GA 30602, USA

Abstract

Super-armed glycosyl donors, whose substituents are predominantly held in pseudoaxial positions, exhibit strongly increased reactivity in glycosylation through significant stabilization of oxocarbenium-like transition states. Examination of X-ray crystal structures reveals that the GH47 family of glycoside hydrolases have evolved so as to distort their substrates away from the ground state conformation in such a manner as to present multiple C-O bonds in pseudoaxial positions and so benefit from conformational super-arming of their substrates, thereby enhancing catalysis. Through analysis of literature mutagenic studies, we show that a suitably placed aromatic residue in GHs 6 and 47 sterically enforces super-armed conformations on their substrates. GH families 45, 81, and 134 on the other hand impose conformational super-arming on their substrates, by maintaining the more active ring conformation through hydrogen bonding rather than steric interactions. The recognition of substrate super-arming by select GH families provides a further parallel with synthetic carbohydrate chemistry and nature and opens further avenues for the design of improved glycosidase inhibitors.

Graphical Abstract

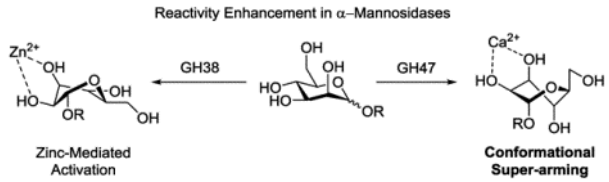

Keywords

Glycoside hydrolases; conformational analysis; super-arming; α-mannosidases; twist-boat; half-chair; CH-π interactions; electrostatic transition state stabilization

David.Crich@uga.edu .

Introduction

Glycoside hydrolases (GHs) are carbohydrate processing enzymes that catalyze the cleavage of glycosidic bonds from either the terminal (exo-GHs) or internal (endo-GHs) positions of saccharides and oligosaccharides. They are found in all kingdoms of life and their absence or malfunction is associated with multiple human disease states, resulting in an immense interest in their mechanisms of action[1–5] and in the design of inhibitors, ideally with selectivity for one class over another so as to limit toxicity.[6–8] Multiple families (~170) of GH exist that, with certain exceptions (GH families 4, 88, 105, and 109),[9–17] proceed by cleavage of the exocyclic glycosidic bond through what are considered to be exploded transition states that involve substantial oxocarbenium ion character, with either inversion or retention (double inversion) of configuration (Figure 1a–c) and the potential for substantial variation in the degree of synchronicity. The mechanisms of chemical glycosidic bond formation and hydrolysis resemble those of GH glycosidic bond hydrolysis in that they also typically proceed with substantial oxocarbenium ion character at the transition state,[18–20] and as such it is not surprising that GHs and glycosyltransferases (GTs) have provided the inspiration for the development of new glycosylation reactions.[21, 22]

In chemical glycosylation it has been established that of the three staggered conformations of the side chain (the exocyclic C5-C6 bond in the hexopyranoses and the C6-C7-bond in the ulosonic and neuraminic acids), the *trans,gauche* (*tg*) conformation destabilizes oxocarbenium-like transition states and so retards reactions, whereas the *gauche,gauche* (*gg*) conformation stabilizes oxocarbenium-like transition states and correspondingly accelerates reactions: the *gauche,trans* (*gt*) conformation displays intermediate behavior.[23] This influence of exocyclic bond conformation on reactivity at the anomeric center arises from the relationship of the C-O bond in the side chain with the nascent positive charge at the transition state, either providing electrostatic stabilization (*gg*, and *gt*) or causing destabilization because of its electron-withdrawing nature (*tg*) (Figure 2 a–c).[24–30] In keeping with the well-established principles of reactivity and the mechanistic parallels between chemical and enzymatic cleavage and formation of C-O bonds at the anomeric center, we recently demonstrated by analysis of available crystallographic data that GHs also employ restriction of side chain conformation to assist catalysis. Thus, an exhaustive search of the PDB with the aid of the Carbohydrate-Active Enzymes Database (CAZy, http://www.cazy.org)[31] revealed that 84% of β-glucosidases, 75% of β-glucosaminidases, 99% of α-glucosidases, and 100% of α-glucosaminidases and β-mannosidases bind their substrates, substrate analogs, or transition state analog inhibitors[1] with their side chains in the reactivity-enhancing *gg* conformation.[32] These strikingly high populations of the *gg* conformation in molecules bound at the active site (−1 site)[33] very significantly exceed those found in free solution (Figure 2a) and in complexes with lectin carbohydrate binding domains. In contrast, galactosidases bind their substrates with a class dependent preference for the *gt* or *tg* conformations, no doubt because of the relatively higher energy of the *gg* conformation in galactosides as reflected in the typical solution phase population distribution (Figure 2b).

The α-mannosidases (found in GHs 31, 38, 47, 63, 76, 92, 99, and 125),[31] however, were found to constitute a broad exception to the very high preference for binding of

the *gg* conformation exhibited by the α- and β-glucosidases and the β-mannosidases.[32] Thus, of the 54 complexes located in the PDB meeting the criteria of ≤ 2.00 Å resolution and conformational integrity as judged by Privateer,[34] 25 had the side chain restricted by hydrogen-bonding to the *gg* and 28 to the *gt* conformations (with the remaining structure taking up an eclipsed conformation), at first sight suggesting that the α-mannosidases do not control side chain conformation to facilitate hydrolysis. Closer examination however revealed that, in point of fact, the 28 structures with the *gt* conformation were limited to only two GH families: 18 from GH38 and 10 from GH47, with all other α-mannosidases following the more typical behavior. Further, among all 170 GH families, only α-mannosidases from these two families together with those from GH92 (where the side chain is bound in the *gg* conformation) employ an essential divalent metal cation that chelates O2 and O3 of the ligand. We sought to understand these family specific exceptions to the broad general rule and present here our findings that Nature has again preempted chemists in the discovery and application of a principle of chemical reactivity, the conformational super-arming principle[6, 35–42] for the stabilization of positive charge in glycosyl oxocarbenium-like transition states, and its application to the catalysis of glycosidic bond cleavage.

Results and Discussion

We first address the GH class 38 and 92 α-mannosidases for which Scheme 1a shows the conformational itinerary through the course of the hydrolysis reaction.[43–47] The former use a retaining mechanism, with an active site aspartate as nucleophile, whereas the latter employ an inverting mechanism with water as a nucleophile. In each, the substrate binds in a ${}^{O}S_2$ twist boat conformation, passes through an approximate $B_{2,5}$ boat-like transition state, and ends in a ${}^{1}S_5$ twist boat as either a covalent glycosyl enzyme intermediate (GH38) or as the hydrolyzed product (GH92).[48]

GH38 mannosidases only bind Zn^{2+} in their active sites. Chelation of O2 and O3 by the metal facilitates twisting of the starting material from the ground state ${}^{4}C_1$ chair to a skew boat closer in character to the $B_{2,5}$ boat-like transition state, as suggested by the Rose and Bols groups in their analysis of binding of the inhibitor noeuromycin.[45] Further, acidification of hydroxyl groups via coordination by Zn^{2+} is well established,[49] with an observed reduction of the pK_a of coordinated water to 9 in free solution and to 6 in carboxypeptidase active sites.[50] Such acidification of O2 and O3 through chelation to Zn^{2+} affords significant transition state stabilization, as these groups are rendered less electron-withdrawing. In the GH38 mannosidases Zn^{2+} also coordinates to the aspartate nucleophile (Figure 3a)[45] presumably orienting it for nucleophilic attack. Apparently, TS stabilization arising from chelation to Zn^{2+} in GH38s is such that no significant benefit is derived from enforcement of the *gg* side chain conformation.

In contrast, chelation to Ca^{2+} is significantly less activating as is apparent from the smaller reduction in the p*K*a of coordinated water to only 12.6.[51, 52] While this does not preclude orientation of catalytic aspartate or glutamate residues, as observed with GH97 glucosidases[53] and with *B. thetaiotaomicron* GH92 mannosidases (Figure 3b),[54] Ca^{2+} does not significantly acidify O2 and O3 of the substrate. Rather, the Ca^{2+} serves principally to

bind the ligand, as it is known to do in multiple lectins,[55] and to orient the nucleophilic water.[44] Consistent with the minimal activation provided by chelation to Ca^{2+}, the Ca^{2+}-dependent GH92 series of mannosidases impose the *gg* conformation of the side chain on their ligands so as to provide additional stabilization to the TS. In contrast to the GH92s, the Ca^{2+} dependent GH47 mannosidases benefit neither from metal-mediated activation of the catalytic aspartate (Figure 3c)[56] nor from enforcement of the *gg* conformation.

The key to the high reactivity of the GH47 mannosidases is revealed by Davies' study of the conformational itinerary followed by their substrates during hydrolysis (Scheme 2a).[57] The substrate binds in a distorted $^{3}S_{1}$ twist boat conformation, where, in contrast with GHs 38 and 92, the substituents at C3, C4, and C5 are all pseudoaxial, as observed with a non-hydrolyzable thioglycoside bound to *Caulobacter sp.* K31 (Scheme 2b). The pseudoaxial orientation of these C-O bonds is maintained over the course of the reaction as the substrate passes through a $^{3}H_{4}$ half chair-like transition state, as seen with the complex of a mannoimidazole bound to the same enzyme (Scheme 2c), to the hydrolyzed product that is held as an "inverted" $^{1}C_{4}$ chair conformation as exhibited by the *Caulobacter* sp. K31 complex with noeuromycin (Scheme 2d).

Further analysis of crystal structures of GH47 mannosidases reveals that a suitably placed aromatic residue (Figure 4)[58] abuts the C4-C5-C6 plane of the bound pyranoside. As previously noted for arenes in the −1 site of the majority of GHs,[59] this arene doubtless stabilizes the Michaelis complex through CH-π interactions,[60] which are accentuated for H5 at the TS due to its proximity to the partial positive charge. We suggest, however, that a major function of this aryl group in proximity to C5 is to enforce distortion of the pyranoside ring at the −1 site away from the $^{4}C_{1}$ chair so as to avoid a steric clash with the hydroxymethyl side chain. This is illustrated by mutagenic studies carried out by the Moremen group,[58] where the F659A mutation in human ER α-mannosidase results in a 140-fold drop in k_{cat}/K_{M} indicating that removal of the steric bulk offered by F659 allows the substrate to take a more relaxed $^{4}C_{1}$ or analogous conformation in the −1 site. Likewise, the F659A mutation results in a 60-fold drop in binding affinity for kifunensine, an inhibitor, whose ground state conformation is an inverted $^{1}C_{4}$ chair, that binds near-irreversibly to the wild type enzyme.

Importantly, the enforcement of the $^{3}H_{4}$ conformation of the substrate at the TS by F659 not only provides a measure of TS stabilization by apposite CH-π interactions but also positions the C3-O3 and C4-O4 bonds of the ligand so as to further stabilize the partial positive charge at the TS through space electrostatically: in the language of preparative carbohydrate chemistry the substrate is super-armed. It has been broadly demonstrated that the greater chemical reactivity of galactopyranosides with respect to their gluco-isomers is mainly due to the through space stabilization of partial positive charge at the TS by the axial C4-O4 bond (Figure 5),[18, 29, 61–65] as most apparent in Bols' linear free energy relationships correlating rates of glycoside hydrolysis with p*K*a's of analogously substituted polyhydroxypiperidines.[29, 66, 67] This is directly analogous to the stabilization provided to the TS by side chains in the *gg* conformation (Figure 2). Extrapolating from this phenomenon, Bols and coworkers revealed dramatic rate increases in glycosidic bond hydrolysis when all C-O bonds are locked in pseudoaxial positions as illustrated by the

~450-fold rate increase seen with methyl 3,6-anhydro-β-D-glucopyranoside as compared to methyl α-D-glucopyransoide (Figure 5b).[35] In preparative chemistry, Bols and others made use of this super-arming effect through the design and application of a series of conformationally distorted donors, with multiple pseudoaxial C-O bonds, that can be preferentially activated in the presence of related donors in the more usual $^4C_1$ conformation (Figure 5c), albeit the situation is obscured in this case by the change in nature of the protecting groups.[37] It appears that the GH47 mannosidases have evolved to distort their substrates away from the ground state conformation so as to position their C3-O3 and C4-O4 bonds in such a manner as to take advantage of super-arming and achieve higher levels of activity.

Enhancement of reactivity through conformational super-arming is not restricted to the GH47 α-mannosidases. In GH6 cellulases, a proximal tyrosine residue whose phenolic OH sterically prevents the substrate from taking up a $^4C_1$ chair conformation forces the sugar into a ^2E half chair or a ^2S_O skew boat with pseudoaxial substituents at C4 and C5 (Figure 6a), to which it also provides the more typical CH-π and/or hydrophobic stabilization.[59] While the tenfold decrease in activity found by Larsson and coworkers with a Y73F mutant of *T. fusca* Cel6A can potentially by attributed to reduced stabilization of nascent positive charge at the anomeric center by the less electron rich arene, a Y73S mutant lacking the steric bulk of an aromatic ring results in a much larger 500-fold decrease in activity.[68, 69] Crystal structures of the Y73S mutant bound to cellotetraose reveal that the pyranoside ring in the −1 site is held in the relaxed $^4C_1$ conformation (Figure 6b), indicating that the tyrosine residue in the wild type enzyme increases reactivity by conformational arming of the substrate in the −1 site in addition to any stabilization it provides directly to the positive charge at the transition state. Interestingly, despite the significant destabilization afforded by placing the side chain above the pyranoside ring, GH6 endoglucanases hold the side chains of the ring undergoing hydrolysis in the *gg* conformation, thereby further maximizing reactivity.

In some cases, such as the GH81 and GH45 endoglucanases and the GH134 β-mannanases, enforcement of super-arming seems to be consistent throughout the family, with most or all available crystal structures binding the ligand in the more reactive conformation. Unlike the GH6 and 47 glycosidases, enforcement of the higher energy super-arming conformation by GHs 45, 81, and 134 is driven predominantly by H-bonding with the enzyme rather than by steric destabilization of the ground state conformation (Figure 7a–c).[70–72] As with GH6, GHs 45 and 134 restrict their side chains to the most reactive *gg* conformation despite the destabilization afforded by placing the side chain directly above the ring. GH81 endoglucanases, on the other hand, avoid this steric penalty and hold their side chains in the *gt* conformation, constituting one of the exceptions discussed in our earlier analysis of enforced side chain conformations.[32] In other families, only one of the crystal structures shows binding of the substrate in the super-armed conformation. For example, while most GH22 lysozymes bind their substrates in the more relaxed $^4C_1$ conformation, one crystal structure of *M. lusoria* GH22 lysozyme reveals a tetrasaccharide-based unsaturated lactone-type inhibitor bound in a ^5E conformation with pseudoaxial bonds at C4 and C5 distinct from the free solution E_5 conformation[73] of such lactones, indicating super-arming of the natural substrate (Figure 7d). Likewise, one crystal structure of a GH48 glucosidase holds

a cellobio-derived isofagomine in the inverted $^1C_4$ chair with the side chain in the *gt* conformation (Figure 7e).

Finally, it is appropriate to compare the rate enhancement provided by super-arming with that achieved by GHs over the uncatalyzed hydrolysis in water. Thus, super-arming provides an ~400-fold enhancement in the rate of hydrolysis of methyl glucosides (Figure 5) corresponding to a reduction in activation energy of ~1.9 kcal.mol^{-1}, whereas GHs are known to accelerate hydrolysis by a factor of 10^{15}–10^{21} over the uncatalyzed reaction in water (19–29 kcal.mol^{-1}).[74] Accordingly, we estimate that conformational super-arming can provide as much as 10% of the rate enhancement in hydrolysis achieved by the GHs that employ it.

Conclusion

We show that GH47 mannosidases and several other GH families impose a super-armed conformation on their substrates to enhance catalysis. Some families, such as GHs 47 and 6, enforce this conformation through steric interactions that favor substrate conformations with pseudoaxial C-O bonds at the 3- and 4-positions as well as a pseudoaxial side chain, whereas other families such as GHs 81, 134, and 45 employ H-bonding as the primary conformation driving factor. As with our previous analyses of side chain conformation preferences, this work illustrates that Nature is yet again one step ahead, having evolved to take advantage of a phenomenon that chemists have only recently discovered and began to exploit.

Acknowledgments:

We thank the NIH (GM62160) for support. Graphics were generated using UCSF Chimera, developed by the Resource for Biocomputing, Visualization, and Informatics at the University of California, San Francisco, with support from NIH P41-GM103311.

References

1. Gloster TM; Davies GJ, Glycosidase Inhibition: Assessing Mimicry of the Transition State. Org. Biomol. Chem 2010, 305–320. [PubMed: 20066263]
2. Zechel DL; Withers SG, Glycosidase Mechanisms: Anatomy of a Finely Tuned Catalyst. Acc. Chem. Res 2000, 33, 11–18. [PubMed: 10639071]
3. Davies GJ; Planas A; Rovira C, Conformational Analyses of the Reaction Coordinate of Glycosidases. Acc. Chem. Res 2012, 45, 308–316. [PubMed: 21923088]
4. Colombo C; Bennet AJ, Probing Transition State Analogy in Glycoside Hydrolase Catalysis. Adv. Phys. Org. Chem 2017, 51, 99–127.
5. Wu L; Armstrong Z; Schröder SP; de Boer C; Artola M; Aerts JMFG; Overkleeft HS; Davies GJ, An Overview of Activity-Based Probes for Glycosidases. Curr. Opin. Chem. Biol 2019, 53, 25–36. [PubMed: 31419756]
6. Bols M; López O; Ortega-Caballero F, Glycosidase Inhibitors: Structure, Activity, Synthesis, and Medical Relevance. In Comprehensive Glycoscience, vol 1, Kamerling J, Ed. Elsevier: Amsterdam, 2007; Vol. 1, pp 815–884.
7. Compain P; Martin OR, Iminosugars: From Synthesis to Therapeutic Applications. Wiley: Chichester, 2007; p 467.
8. Compain P, Multivalent Effects in Glycosidase Inhibition: The End of the Beginning. Chem. Rec 2020, 20, 10–22. [PubMed: 30993894]

9. Yip VLY; Withers SG, Mechanistic Analysis of the Unusual Redox-Elimination Sequence Employed by *Thermotoga maritima* Bg1T: A 6-Phospho-β-glucosidase from Glycoside hydrolase Family 4. Biochemistry 2006, 45, 571–580. [PubMed: 16401086]
10. Yip VLY; Thompson J; Withers SG, Mechanism of GlvA from *Bacillus subtilis*: A Detailed Kinetic Analysis of a 6-Phospho-α-Glucosidase from Glycoside Hydrolase Family 4. Biochemistry 2007, 46, 9840–9852. [PubMed: 17676871]
11. Liu QP; Sulzenbacher G; Yuan H; Bennett EP; Pietz G; Saunders K; Spence J; Niudelman E; Levery SB; White T; Neveu JM; Lane WS; Bourne Y; Olsson ML; Henrissat B, Bacterial Glycosidases for the Production of Universal Red Blood Cells. Nat. Biotechnol 2007, 25, 454–464. [PubMed: 17401360]
12. Itoh T; Hashimoto W; Mikami B; Murata K, Crystal Structure of Unsaturated Glucuronyl Hydrolase Complexed with Substrate: Molecular Insights into its Catalytic Reaction Mechanism. J. Biol. Chem 2006, 281, 29807–29816. [PubMed: 16893885]
13. Jongkees SAK; Withers SG, Glycoside Cleavage by a New Mechanism in Unsaturated Glucuronyl Hydrolases. J. Am. Chem. Soc 2011, 133, 19334–19337. [PubMed: 22047074]
14. Jongkees SAK; Yoo H; Withers SG, Mechanistic Investigations of Unsaturated Glucuronyl Hydrolase from *Clostridium perfringens*. J. Biol. Chem 2014, 289, 11385–11395. [PubMed: 24573682]
15. Itoh T; Ochiai A; Mikami B; Hashimoto W; Murata K, A Novel Glycoside Hydrolase Family 105: The Structure of Family 105 Unsaturated Rhamnogalacturonyl Hydrolase Complexed with a Disaccharide in Comparison with Family 88 Enzyme Complexed with the Disaccharide. J. Mol. Biol 2006, 360, 573–585. [PubMed: 16781735]
16. Jongkees SAK; Withers SG, Unusual Enzymatic Glycoside Cleavage Mechanisms. Acc. Chem. Res 2014, 47, 226–235. [PubMed: 23957528]
17. Collén PN; Jeudy A; Sassi J-F; Groisillier A; Czjzek M; Coutinho PM; Helbert W, A Novel Unsaturated β-Glucuronyl Hydrolase Involved in Ulvan Degradation Unveils the Versatility of Stereochemistry Requirements in Family GH105. J. Biol. Chem 2014, 289, 6199–6211. [PubMed: 24407291]
18. Adero PO; Amarasekara H; Wen P; Bohé L; Crich D, The Experimental Evidence in Support of Glycosylation Mechanisms at the S_N1-S_N2 Interface. Chem. Rev 2018, 118, 8242–8284. [PubMed: 29846062]
19. Hettikankanamalage A; Lassfolk R; Ekholm F; Leino R; Crich D, Mechanisms of Stereodirecting Participation and Ester Migration from Near and Far in Glycosylation and Related Reactions. Chem. Rev 2020, 120, 7104–7151. [PubMed: 32627532]
20. Crich D, En Route to the Transformation of Glycoscience: A Chemist's Perspective on Internal and External Crossroads in Glycochemistry. J. Am. Chem. Soc 2021, 143, 17–34. [PubMed: 33350830]
21. Park Y; Harper KC; Kuhl N; Kwan EE; Liu RY; Jacobsen EN, Macrocyclic Bis-Thioureas Catalyze Stereospecific Glycosylation Reactions. Science 2017, 355, 162–166. [PubMed: 28082586]
22. Peng P; Schmidt RR, Acid–Base Catalysis in Glycosidations: A Nature Derived Alternative to the Generally Employed Methodology. Acc. Chem. Res 2017, 50, 1171–1183. [PubMed: 28440624]
23. Side chain conformations are described by a nomenclature in which the first of the two descriptors pertains to the relationship between the C5-O5 bond in the ring oxygen and the C6-O6 bond at the exocyclic carbon (*gauche* or *trans*), while the second descriptor describes the relationship of the C6-O6 bond and the exocylic carbon to the C5-C4 bond.
24. Jensen HH; Nordstrøm LU; Bols M, The Disarming Effect of the 4,6-Acetal Group on Glycoside Reactivity: Torsional or Electronic. J. Am. Chem. Soc 2004, 126, 9205–9213. [PubMed: 15281809]
25. Moumé-Pymbock M; Furukawa T; Mondal S; Crich D, Probing the Influence of a 4,6-*O*-Acetal on the Reactivity of Galactopyranosyl Donors: Verification of the Disarming Influence of the *trans-gauche* Conformation of C5-C6 Bonds. J. Am. Chem. Soc 2013, 135, 14249–14255. [PubMed: 23984633]

26. Kancharla PK; Crich D, Influence of Side Chain Conformation and Configuration on Glycosyl Donor Reactivity and Selectivity as Illustrated by Sialic Acid Donors Epimeric at the 7-Position. J. Am. Chem. Soc 2013, 135, 18999–19007. [PubMed: 24261615]
27. Dhakal B; Buda S; Crich D, Stereoselective Synthesis of 5-Epi-α-Sialosides Related to the Pseudaminic Acid Glycosides. Reassessment of the Stereoselectivity of the 5-Azido-5-deacetamidosialyl Thioglycosides and Use of Triflate as Nucleophile in the Zbiral Deamination of Sialic Acids. J. Org. Chem 2016, 81, 10617–10630. [PubMed: 27806203]
28. Dhakal B; Crich D, Synthesis and Stereocontrolled Equatorially Selective Glycosylation Reactions of a Pseudaminic Acid Donor: Importance of the Side Chain Conformation, and Regioselective Reduction of Azide Protecting Groups. J. Am. Chem. Soc 2018, 140, 15008–15015. [PubMed: 30351022]
29. Jensen HH; Bols M, Stereoelectronic Substituent Effects. Acc. Chem. Res 2006, 39, 259–265. [PubMed: 16618093]
30. Smith DM; Woerpel KA, Electrostatic Interactions in Cations and their Importance in Biology and Chemistry. Org. Biomol. Chem 2006, 4, 1195–1201. [PubMed: 16557303]
31. Lombard V; Golaconda RH; Drula E; Coutinho PM; Henrissat B, The Carbohydrate-Active Enzymes Database (CAZy) in 2013. Nucleic Acids Res. 2013, 42, D490–D495. [PubMed: 24270786]
32. Quirke JCK; Crich D, Glycoside Hydolases Restrict the Side Chain Conformation of their Substrates to Gain Additional Transition State Stabilization. J. Am. Chem. Soc 2020, 142, 16965–16973. [PubMed: 32877175]
33. Davies GJ; Wilson KS; Henrissat B, Nomenclature for Sugar-Binding Subsites in Glycosyl Hydrolases. Biochem. J 1997, 321, 557–559. [PubMed: 9020895]
34. Agirre J; Iglesias-Fernández J; Rovira C; Davies GJ; Wilson KS; Cowtan K, Privateer: Software for the Conformational Validation of Carbohydrate Structures. Nat. Struct. Biol 2015, 22, 833–834.
35. McDonnell C; López O; Murphy PV; Fernández Bolaños JG; Hazell RG; Bols M, Conformational Effects on Glycoside Reactivity: Study of the High Reactive Conformer of Glucose. J. Am. Chem. Soc 2004, 126, 12374–12385. [PubMed: 15453771]
36. Jensen HH; Pedersen CM; Bols M, Going to Extremes: “Super” Armed Glycosyl Donors in Glycosylation Chemistry. Chem. Eur, J 2007, 13, 7576–7582. [PubMed: 17705330]
37. Pedersen CM; Nordstrom LU; Bols M, “Super Armed” Glycosyl Donors: Conformational Arming of Thioglycosides by Silylation J. Am. Chem. Soc 2007, 129, 9222–9235. [PubMed: 17602482]
38. Pedersen CM; Marinescu LG; Bols M, Conformationally Armed Glycosyl Donors: Reactivity Quantification, New Donors and One Pot Reactions. Chem. Commun 2008, 2465–2467.
39. Pedersen CM; Marinescu LG; Bols M, Glycosyl Donors in Unusual Conformations - Influence on Selectivity and Reactivity. Comptes Rendus Chimie 2011, 14, 17–43.
40. Heuckendorff M; Premathilake HD; Pornsuriyasak P; Madsen AO; Pedersen CM; Bols M; Demchenko AV, Superarming of Glycosyl Donors by Combined Neighboring and Conformational Effects. Org. Lett 2013, 15, 4904–4907. [PubMed: 24006853]
41. Okada Y; Mukae T; Okajimia K; Taira M; Fujita M; Yamada H, Highly β-Selective *O*-Glucosidation Due to the Restricted Twist-Boat Conformation. Org. Lett 2007, 9, 1573–1576. [PubMed: 17358075]
42. Okada Y; Nagata O; Taira M; Yamada H, Highly β-Selective and Direct Formation of 2-*O*-Glycosylated Glucosides by Ring Restriction into Twist Boat. Org. Lett 2007, 9, 2755–2758. [PubMed: 17602562]
43. Rovira C; Males A; Davies GJ; Williams SJ, Mannosidase Mechanism: At the Intersection of Conformation and Catalysis. Curr. Opin. Struct. Biol 2020, 62, 79–92. [PubMed: 31891872]
44. Zhu Y; Suits MDL; Thompson AJ; Chavan S; Dinev Z; Dumon C; Smith N; Moremen KW; Xiang Y; Siriwardena A; Williams SJ; Gilbert HJ; Davies GJ, Mechanistic Insights Into a Ca^{2+}-Dependent Family of Alpha-Mannosidases in a Human Gut Symbiont. Nat. Chem. Biol 2010, 6, 125–132. [PubMed: 20081828]

45. Kuntz DA; Liu H; Bols M; Rose DR, The Role of the Active Site Zn in the Catalytic Mechanism of the GH38 Golgi α-Mannosidase II: Implications from Noeuromycin Inhibition. Biocatal. Biotransformation 2006, 24, 55–61.
46. Williams RJ; Iglesias-Fernández J; Stepper J; Jackson A; Thompson AJ; Lowe EC; White JM; Gilbert HJ; Rovira C; Davies GJ; Williams SJ, Combined Inhibitor Free-Energy Landscape and Structural Analysis Reports on the Mannosidase Conformational Coordinate. Angew. Chem. Int. Ed 2014, 53, 1087–1091.
47. Kuntz DA; Tarling CA; Withers SG; Rose DR, Structural Analysis of Golgi α-Mannosidase II Inhibitors Identified from a Focused Glycosidase Inhibitor Screen. Biochemistry 2008, 47, 10058–10068. [PubMed: 18759458]
48. Complexes of transition state analogs with enzyme active sites are stable complexes and consequently are only approximations of the actual transition state structures with their partial bonds and charges. Schramm VL Acc. Chem. Res 2015, 48, 1032–1039. [PubMed: 25848811]
49. Lipscomb WN; Sträter N, Recent Advances in Zinc Enzymology. Chem. Rev 1996, 96, 2375–2434. [PubMed: 11848831]
50. Mock WL; Freeman DJ; Aksamawati M, Fluxionate Lewis Acidity of the Zn2+ Ion in Carboxypeptidase A. Biochem. J 1993, 289, 185–193. [PubMed: 8424757]
51. Kumar A; Blakemore JD, On the Use of Aqueous Metal-Aqua pKa Values as a Descriptor of Lewis Acidity. Inorg. Chem 2021, 60, 1107–1115. [PubMed: 33405902]
52. Perrin DD, Ionisation Constants of Inorganic Acids and Bases in Aqueous Solution. Pergamon: 1982.
53. Okuyama M; Yoshida T; Hondoh H; Mori H; Yao M; Kimura A, Catalytic Role of the Calcium Ion in GH97 Inverting Glycoside Hydrolase. FEBS Lett. 2014, 588, 3213–3217. [PubMed: 25017438]
54. Thompson AJ; Spears RJ; Zhu Y; Suits MDL; Williams SJ; Gilbert HJ; Davies GJ, *Bacteroides thetaiotaomicron* Generates Diverse α-Mannosidase Activities Through Subtle Evolution of a Distal Substrate-Binding Motif. Acta Crystallogr. D 2018, 74, 394–404.
55. Imberty A; Mitchell EP; Wimmerová M, Structural Basis of High-Affinity Glycan Recognition by Bacterial and Fungal Lectins. Curr. Opin. Struct. Biol 2005, 15, 525–534. [PubMed: 16140523]
56. Vallée F; Karaveg K; Herscovics A; Moremen KW; Howell PL, Structural Basis for Catalysis and Inhibition of N-Glycan Processing Class I α-1,2-Mannosidases. J. Biol. Chem 2000, 275, 41287–41298. [PubMed: 10995765]
57. Thompson AJ; Dabin J; Iglesias-Fernandez J; Ardevol A; Dinev Z; Williams SJ; Bande O; Siriwardena A; Moreland C; Hu T-C; Smith DK; Gilbert HJ; Rovira C; Davies GJ, The Reaction Coordinate of a Bacterial GH47 α-Mannosidase: A Combined Quantum Mechanical and Structural Approach. Angew. Chem. Int. Ed 2012, 51, 10997–11001.
58. Karaveg K; Moremen KW, Energetics of Substrate Binding and Catalysis by Class 1 (Glycosylhydrolase Family 47) α-Mannosidases Involved in N-Glycan Processing and Endoplasmic Reticulum Quality Control. J. Biol. Chem 2005, 280, 29837–29848. [PubMed: 15911611]
59. Nerinckx W; Desmet T; Claeyssens M, A Hydrophobic Platform as a Mechanistically Relevant Transition State Stabilising Factor Appears to be Present in the Active Centre of All Glycoside Hydrolases. FEBS Lett. 2003, 538, 1–7. [PubMed: 12633843]
60. Hudson KL; Bartlett GJ; Diehl RC; Agirre J; Gallagher T; Kiessling LL; Woolfson DN, Carbohydrate–Aromatic Interactions in Proteins. J. Am. Chem. Soc 2015, 137, 15152–15160. [PubMed: 26561965]
61. Namchuk MN; McCarter JD; Becalski A; Andrews T; Withers SG, The Role of Sugar Substituents in Glycoside Hydrolysis. J. Am. Chem. Soc 2000, 122, 1270–1277.
62. Miljkovic M; Yeagley D; Deslongchamps P; Dory YL, Experimental and Theoretical Evidence of Through-Space Electrostatic Stabilization of the Incipient Oxocarbenium Ion by an Axially Oriented Electronegative Substituent During Glycopyranoside Acetolysis. J. Org. Chem 1997, 62, 7597–7604.
63. Woods RJ; Andrews CW; Bowen JP, Molecular Mechanical Investigations of the Properties of Oxacarbenium Ions. Application to Glycoside Hydrolysis. J. Am. Chem. Soc 1992, 114, 859–864.

64. Bülow A; Meyer T; Olszewski TK; Bols M, The C-4 Configuration as a Probe for the Study of Glycosidation Reactions. Eur. J. Org. Chem 2004, 323–329.

65. Jensen HH; Bols M, Steric Effects Are Not the Cause of the Rate Difference in Hydrolysis of Stereoisomeric Glycosides. Org. Lett 2003, 5, 3419–3421. [PubMed: 12967289]

66. Jensen HH; Lyngbye L; Bols M, A Free Energy Relationship between the Rate of Acidic Hydrolysis of Glycosides and the pKa of Isofagamines. Angew. Chem. Int. Ed 2001, 40, 3447–3449.

67. Bols M; Liang X; Jensen HH, Equatorial Contra Axial Polar Substitutents. The Relationship of a Chemical Reaction to Stereochemical Substitutent Constants. J. Org. Chem 2002, 67, 8970–8974. [PubMed: 12467416]

68. Larsson AM; Bergfors T; Dultz E; Irwin DC; Roos A; Driguez H; Wilson DB; Jones TA, Crystal Structure of *Thermobifida fusca* Endoglucanase Cel6A in Complex with Substrate and Inhibitor: The Role of Tyrosine Y73 in Substrate Ring Distortion. Biochemistry 2005, 44, 12915–12922. [PubMed: 16185060]

69. Wolfgang DE; Wilson DB, Mechanistic Studies of Active Site Mutants of *Thermomonospora fusca* Endocellulase E2. Biochemistry 1999, 38, 9746–9751. [PubMed: 10423254]

70. Nakamura A; Ishida T; Kusaka K; Yamada T; Fushinobu S; Tanaka I; Kaneko S; Ohta K; Tanaka H; Inaka K; Higuchi Y; Niimura N; Samejima M; Igarashi K, "Newton's Cradle" Proton Relay with Amide–Imidic Acid Tautomerization in Inverting Cellulase Visualized by Neutron Crystallography. Sci. Adv 2015, 1, e1500263. [PubMed: 26601228]

71. Pluvinage B; Fillo A; Massel P; Boraston AB, Structural Analysis of a Family 81 Glycoside Hydrolase Implicates Its Recognition of β−1,3-Glucan Quaternary Structure. Structure 2017, 25, 1348–1359.e3. [PubMed: 28781080]

72. Jin Y; Petricevic M; John A; Raich L; Jenkins H; Portela De Souza L; Cuskin F; Gilbert HJ; Rovira C; Goddard-Borger ED; Williams SJ; Davies GJ, A β-Mannanase with a Lysozyme-like Fold and a Novel Molecular Catalytic Mechanism. ACS Cent. Sci 2016, 2, 896–903. [PubMed: 28058278]

73. Pravdic N; Danilov B; Fletcher HG, The Oxidation of Partially Protected 2-Acetamido-2-deoxypyranoses with Silver Carbonate on Celite. Carbohydr. Res 1974, 36, 167–180.

74. Wolfenden R; Yuan Y, Rates of Spontaneous Cleavage of Glucose, Fructose, Sucrose, and Trehalose in Water, and the Catalytic Proficiencies of Invertase and Trehalase. J. Am. Chem. Soc 2008, 130, 7548–7549. [PubMed: 18505259]

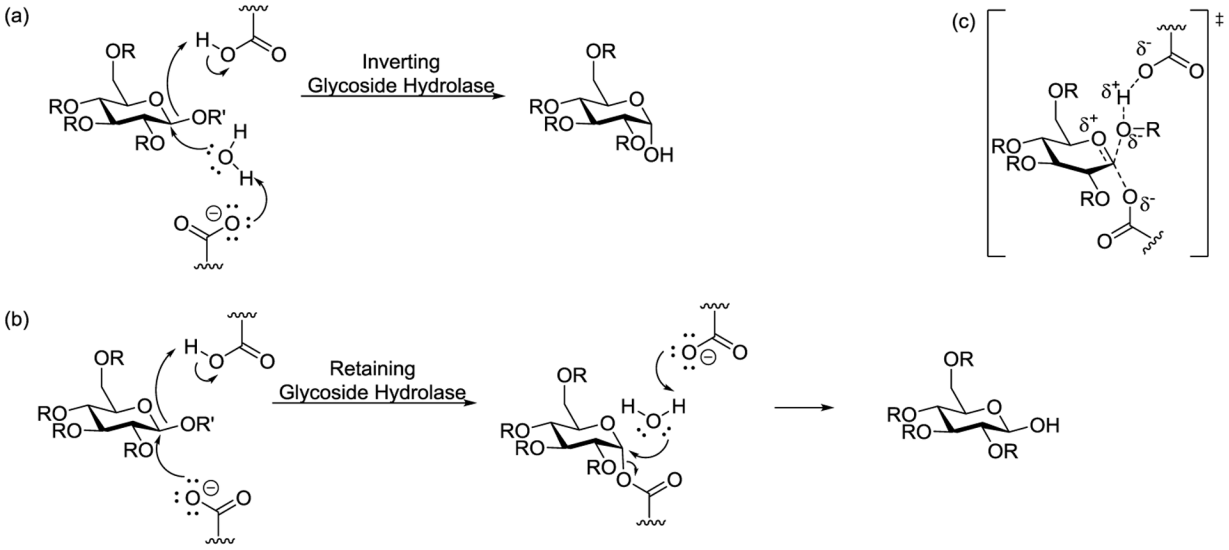

Figure 1.

(a) Mechanism of inverting glycoside hydrolases (b) Mechanism of retaining glycoside hydrolases (c) Concerted oxocarbenium-like transition state for an inverting glycosidase

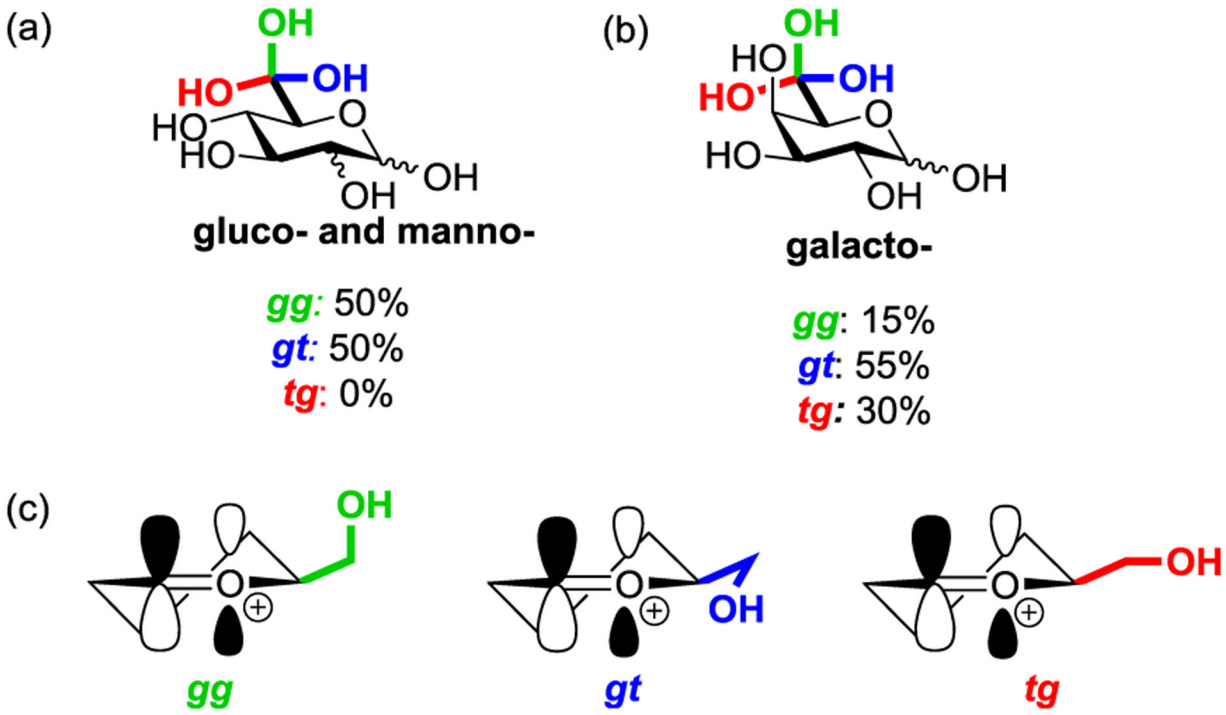

Figure 2.

The three staggered side chain conformations and their approximate populations in free solution for (a) gluco- and mannopyranoses, and (b) for galactopyranoses. (c) Spatial relationships of side chain hydroxyl groups with the putative oxocarbenium π* orbital

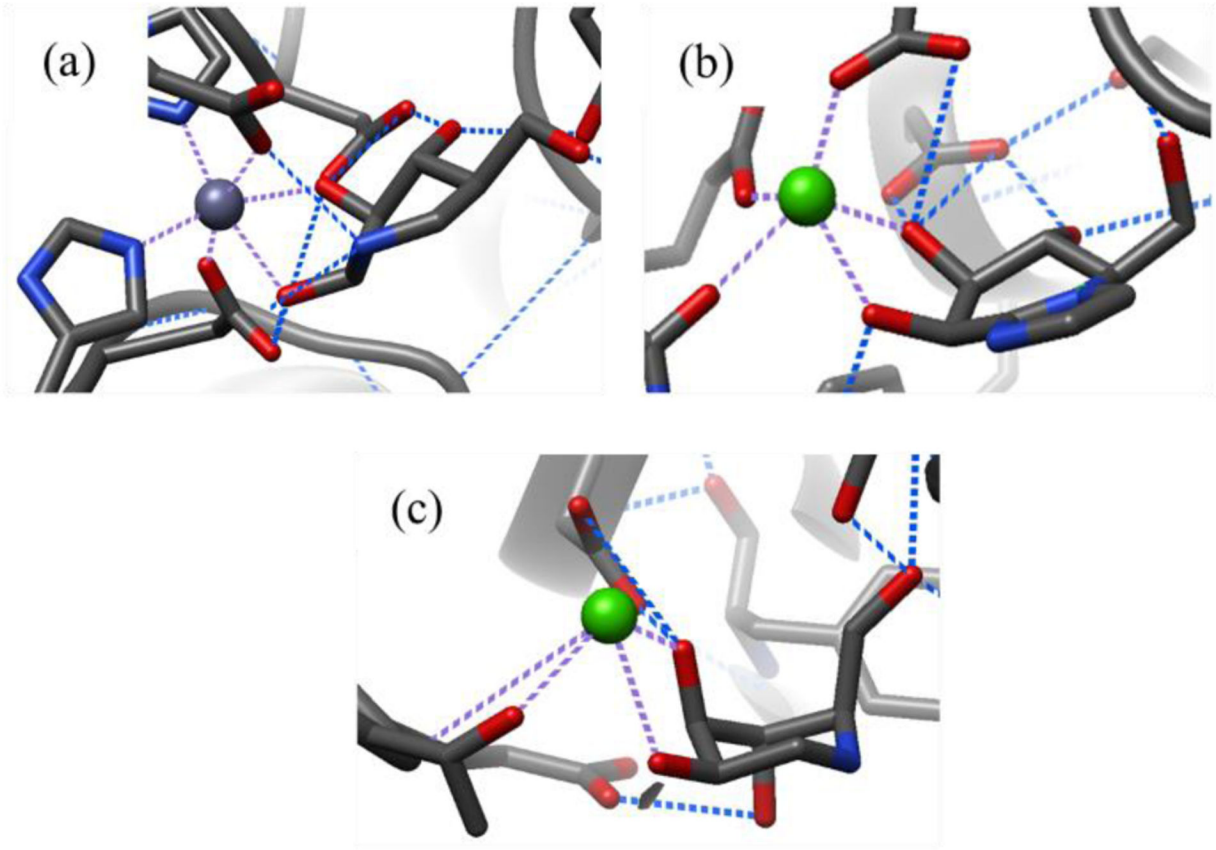

Figure 3.

Coordination spheres of the divalent cation of (a) *D. melanogaster* GH38 golgi α-mannosidase II in complex with a mannoimidazole (Zn^{2+}, PDB ID 2ALW), (b) *B. thetaiotaomicron* GH92 α-1,2-mannosidase in complex with a mannoimidazole (Ca^{2+}, PDB ID 6F92), and (c) human GH47 α-1,2-mannosidase in complex with 1-deoxynojirimycin (Ca^{2+}, PDB ID 1FO2). Blue dashed lines designate hydrogen bonds and purple dashed lines designate coordinative bonds to the metal.

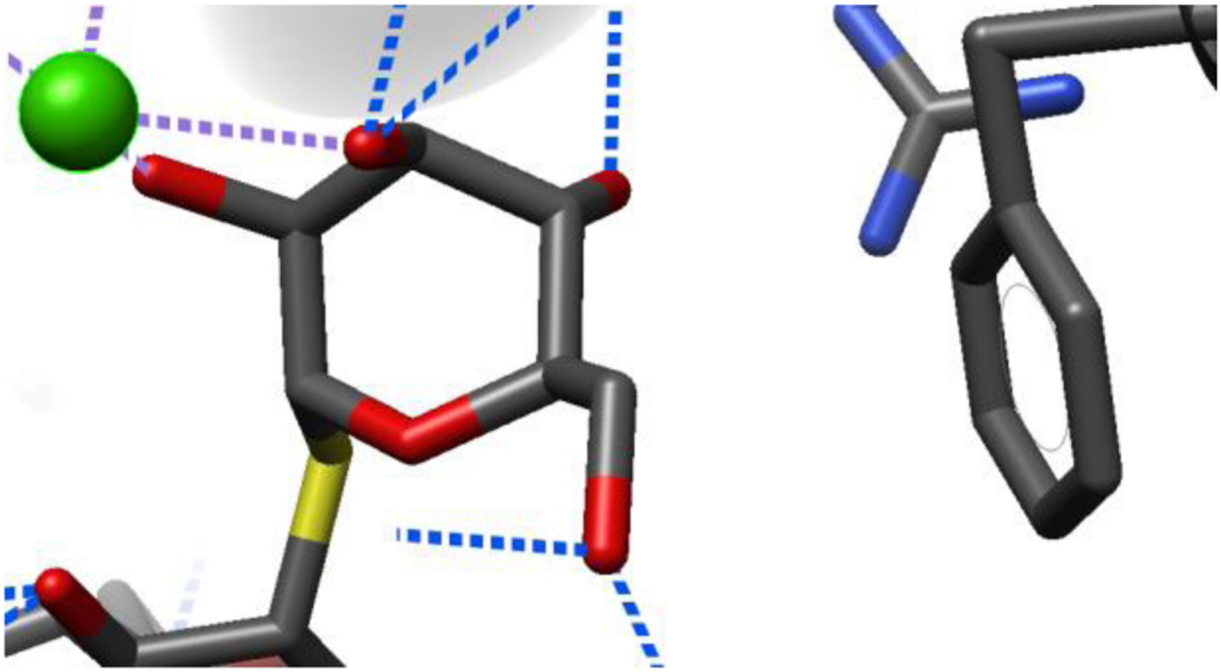

Figure 4.

Partial crystal structure of human GH47 α-1,2-mannosidase bound to thiomannobiose, with F659 abutting the C4-C5-C6 plane (PDB ID 1X9D). Blue dashed lines designate hydrogen bonds and purple dashed lines designate coordinative bonds to the metal.

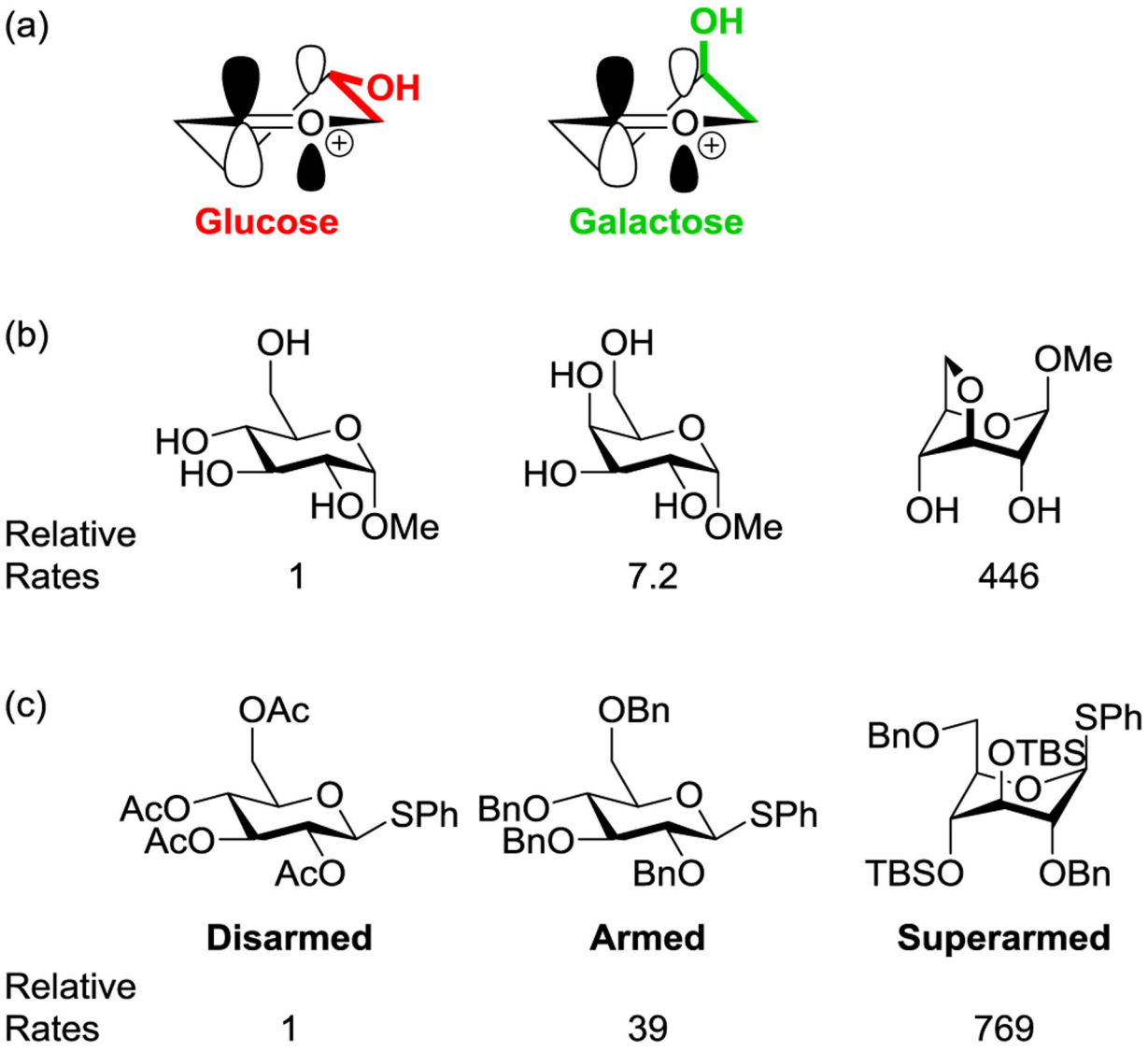

Figure 5.

(a) Impacts of C4 configuration on putative oxocarbenium stability (b) Relative rates of acidic hydrolysis of methyl glycosides with increasing axial character (c) Relative rates of activation of disarmed, armed, and super-armed glycosyl donors[38]

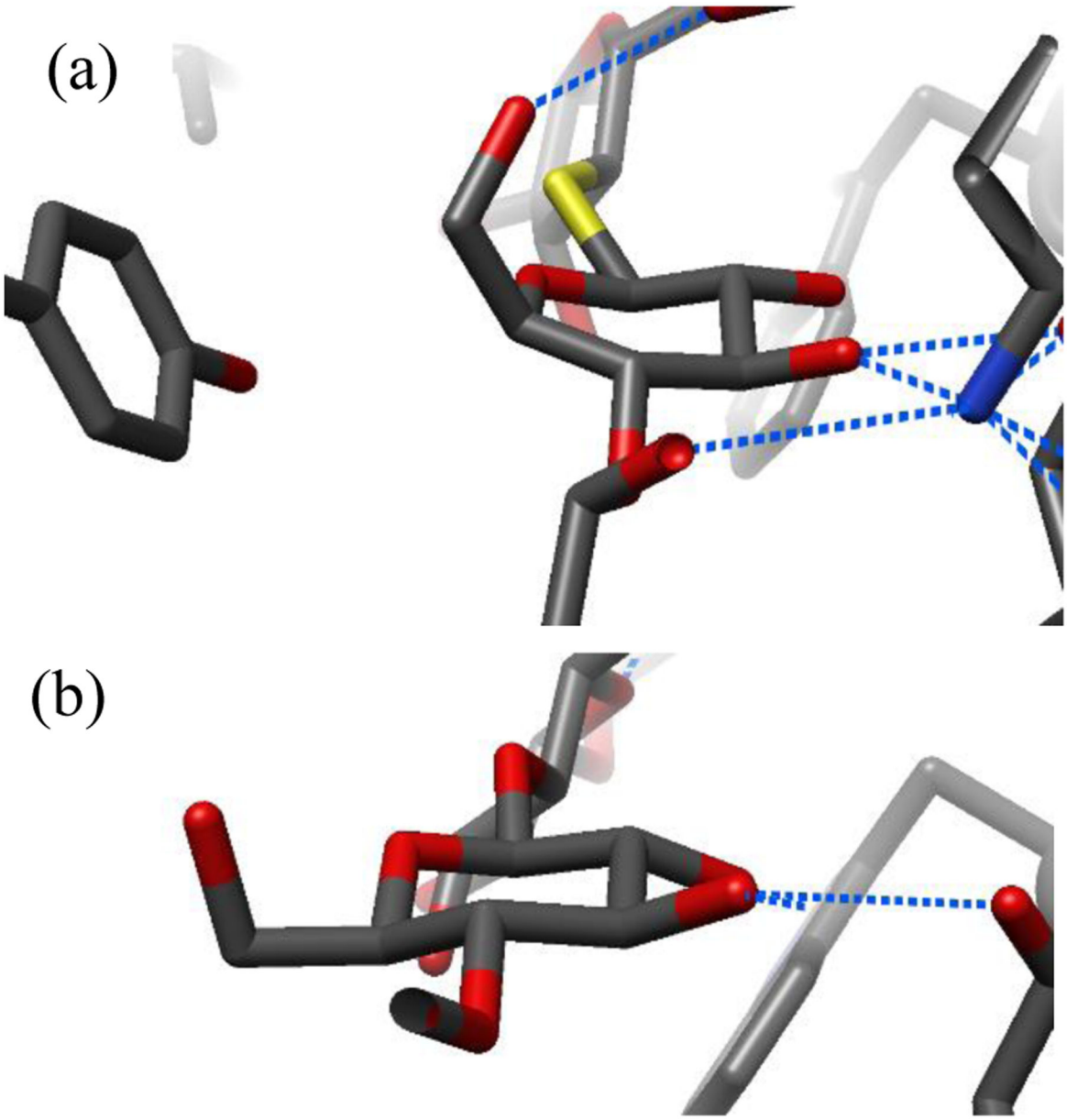

Figure 6.

Partial crystal structures of (a) wild type *T. fusca* GH6 endoglucanase in complex with a thioglycoside (PDB ID 2BOD) and (b) Y73A *T. fusca* GH6 endoglucanase in complex with cellotetraose (PDB ID 2BOF) showing the pyranoside ring in the −1 site. Blue dashed lines designate hydrogen bonds.

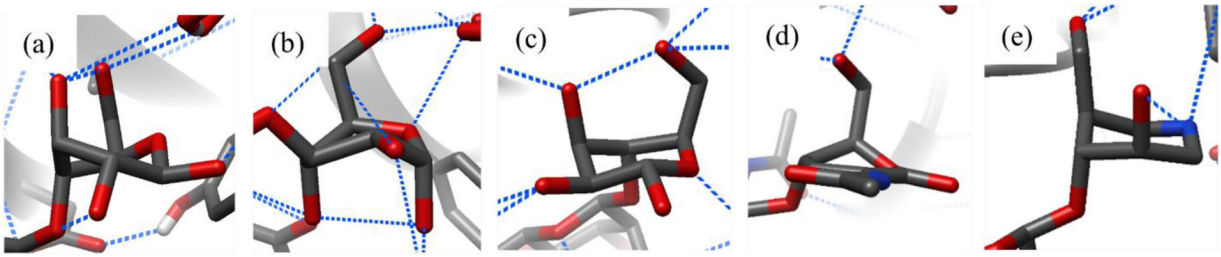

Figure 7.

Partial crystal structures of (a) *P. chryosporum* GH45 endoglucanase bound to cellopentaose (PDB ID 3X2M), (b) *B. halodurans* GH81 glucosidase bound to laminarin (PDB ID 5T4G), (c) *Streptomyces sp*. GH134 β-mannanase bound to mannotriose (PDB ID 5JU9), (d) *M. lusoria* GH22 lysozyme bound to a tetrasaccharide-based unsaturated lactone (PDB ID 3AYQ), and (e) *B. pumilus* GH48 endoglucanase cellobiose-derived isofagomine (PDB ID 5VMA). Blue dashed lines designate hydrogen bonds.

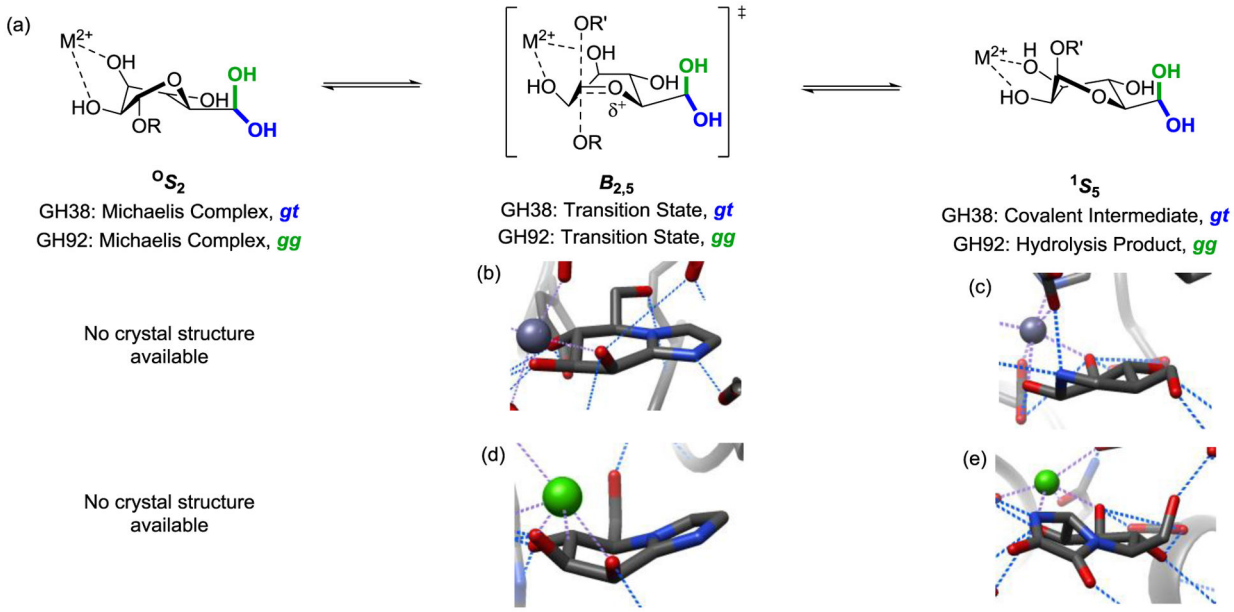

Scheme 1.

(a) Conformational itinerary of pyranosides at the −1 site of GH38 and GH92 mannosidases with partial crystal structures of (b) *D. melanogaster* GH38 Golgi α-1,2-mannosidase bound to a mannoimidazole TS analog inhibitor (PDB ID 3D4Y), (c) *D. melanogaster* GH38 Golgi α-1,2-mannosidase bound to noeuromycin (PDB ID 2ALW), (d) *B. thetaiotaomicron* 3990 GH92 α-mannosidase bound to a mannoimidazole TS analog inhibitor (PDB ID 2WZS), and (e) *B. thetaiotaomicron* 3990 GH92 α-mannosidase bound to kifunensine (PDB ID 2WVZ). Blue dashed lines designate hydrogen bonds and purple dashed lines designate coordinative bonds to the metal.

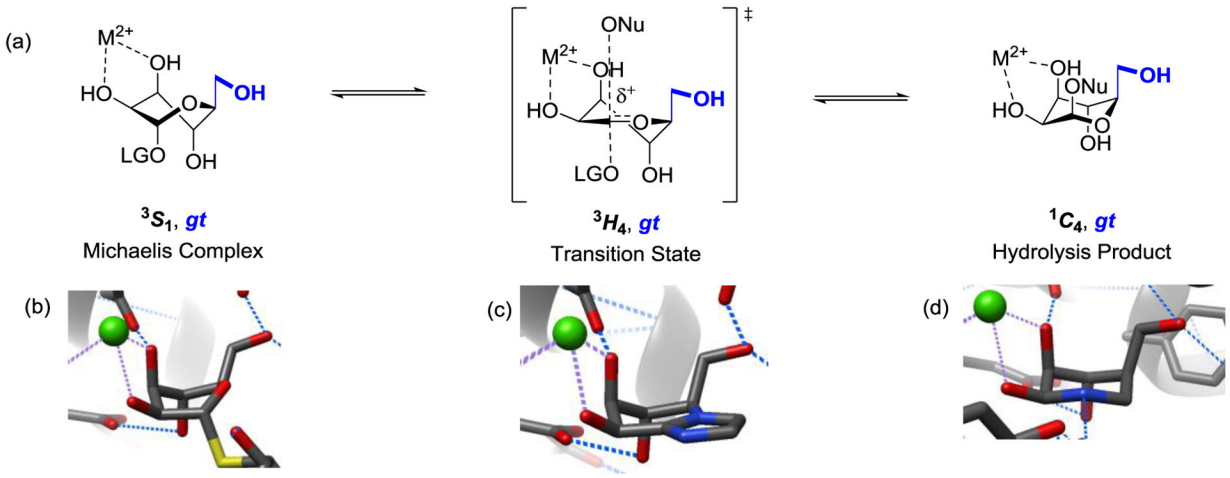

Scheme 2.

(a) Conformational itinerary of pyranosides at the −1 site of GH47 mannosidases, illustrated with partial crystal structures of *Caulobacter sp.* K31 in complex with (b) a thioglycoside (PDB ID 4AYP), (c) a mannoimidazole (PDB ID 4AYQ) 5KK7, and (d) noeuromycin (PDB ID 4AYR). Blue dashed lines designate hydrogen bonds and purple dashed lines designate coordinative bonds to the metal.